RESEARCH ARTICLE | JULY 10 2023

Formulating waterless biocarbon-based masker towards environmental sustainability: Characterizing its functionality

Hanis Nadhirah Eisa; Saiyidah Fatimah Az-Zahidah Norazlee; Irene Tan Jia Lin; Gan Suteng; Palsan Sannasi Abdullah ✉; Siti Nuurul Huda Mohammad Azmin; Hasnah Zakaria

AIP Conference Proceedings 2785, 060003 (2023)
https://doi.org/10.1063/5.0148037

Formulating Waterless Biocarbon-Based Masker Towards Environmental Sustainability: Characterizing Its Functionality

Hanis Nadhirah Eisa[1, a)], Saiyidah Fatimah Az-Zahidah Norazlee[1, b)], Irene Tan Jia Lin[1, c)], Gan Suteng[1, d)], Palsan Sannasi Abdullah[1, e)], Siti Nuurul Huda Mohammad Azmin[1, f)] and Hasnah Zakaria[2, g)]

[1]*Faculty of Agro Based Industry, Universiti Malaysia Kelantan, Jeli Campus, 17600 Jeli, Kelantan, Malaysia.*
[2]*I Medikel Cosmeceutical (M) Sdn Bhd, BK4, Kawasan Industri MARA, Jalan Padang Tembak, Pengkalan Chepa, 16100 Kota Bharu, Kelantan, Malaysia.*

[a)] honeysnadhirah97@gmail.com
[b)] saiyidahfatimah36@gmail.com
[c)] jialinirene95@gmail.com
[d)] gsteng0333@gmail.com
[e)] Corresponding author: palsan.abdullah@umk.edu.my
[f)] huda.ma@umk.edu.my
[g)] hascbk_31@yahoo.com.my

Abstract. Waterproof makeup has an everlasting effect, but difficult to remove and the residues can cause irritation and skin breakout. The use of oil-based makeup remover leaves the skin oily and requires further cleansing. Personal care and cosmetic industries evolve over time with new products coming into the growing market. This is often accompanied by thematic play such as nature inspired and more recently waterless beauty. This paper characterizes the inclusion of a surface modified new biocarbon composite (NBC) in formulating waterless masker that can cleanse, scrub, and at the same time be eco-friendly towards environmental sustainability. The parameters that influence the removal of makeup foundation (MF) up to 88.07% by NBC were determined through Box-Behnken experimental approach, i.e., adsorbent dosage (0.028 g), MF concentration (up to 300 mg/L), particle size (151-300 μm), and contact time (15 min). The kinetic model obeyed the pseudo second-order reaction (R^2= 0.9993). New peaks were observed in the FTIR spectra of NBC that was subjected to makeup removal. The best NBC infused waterless masker formulation (S10) displayed acceptable pH (5-7), stable odour, colour, and texture properties, was easily rinseable, and gentle on the skin. Microbial growth was not observed after 2 weeks storage at room temperature. Less effort was needed for removing makeup as the number of rubs were reduced by 52-58% in comparison to just water, and commercial water-based charcoal face masker. Incorporation of NBC into various personal care product formulation such as cleansing balm, clay mask, face scrub, and shampoo can raise the competitiveness of local product line.

INTRODUCTION

One of the largest consumer market segments in terms of growth, volume, and revenue can be attributed to the beauty and personal care industry. Globally, the market was valued at US$422.72 billion in 2020, and expected to reach US$558.12 billion by the year 2026, with a compound annual growth rate (CAGR) of 4.82% [1]. The beauty care market is dominated by makeup and color cosmetic that commands 60% of the market share driven by consumer aspirations towards more diversified beauty products. Revenues for beauty and personal care products market in Malaysia are projected to reach US$2.5 billion in 2021 with a CAGR of 4% through 2025 [2]. This is a marked increase compared to the US$2.24 billion trade volume for cosmetic and personal care products recorded in 2015 [3].

7th International Conference on Environment 2021 (ICENV2021)
AIP Conf. Proc. 2785, 060003-1–060003-23; https://doi.org/10.1063/5.0148037
Published by AIP Publishing. 978-0-7354-4573-4/$30.00

Among the sales, skin care and makeup categories had the greatest demand and the most advanced growing market with a total import value of US$292 million. The same report noted that United States (US) export to Malaysia increased in 2020 despite the pandemic, which included essential oils, skin care products, cleansers and soaps, and cosmetics ingredients. Local average revenue per user (ARPU) currently amounts to about RM190.

Personal care and cosmetic industries evolve over time with new improved products being introduced into the growing market. This is often accompanied by thematic play such as nature inspired, eco-friendly, and more recently waterless beauty underlying the concern towards environmental sustainability. Increased consumption of water can be observed during the manufacturing of water-based products. This is evident from its the ingredients which usually lists water as aqua. In Euromonitor's 2016 Beauty Survey, 'water-efficient to use and produce', was in fact the most desired green features for 12.5% global respondents compared to recyclable packaging or sustainably sourced ingredients [4]. Apart from consumption matters, water rich products are more prone to spoilage resulting from microbial activity. Thus, inclusion of anti-microbial compounds and preservatives are needed. Waterless formulations are less susceptible to microbial growth due to lower water activity (a_w). Microbial growth thrives at water activity reading above 0.90 (on a scale of 0-1.0). In addition, bound water in masker or lotions can dehydrate or cause dehydration to/ of the skin through repeated daily use. Conversely, the water (aqua) content in a formulation of cleansing bar, for example can be reduced to 5%-10% from 50%-75% and produced by press method [4]. Nevertheless, formulating waterless or products with low water content is a challenge in terms of production and providing the sensorial characteristics feel to consumers.

Makeup products include foundations, face powder, blusher, eye shadow, mascara, eyebrow pencil and the like. Most beauty enhancing and makeup products are waterproof. Waterproof makeup presents a more striking and everlasting effect, but difficult to remove. The residues leftover after normal rinsing with water can cause irritation and skin breakout. The use of oil-based makeup remover leaves the skin oily and requires further cleansing. Other alcohol-based makeup remover also causes skin dehydration. Here we present our attempt in formulating a multifunctional biocarbon-based waterless masker for skincare application, for routine cleansing and makeup removal.

Daily exposure to smoke, smog, and other air pollutants ranging from particulate matter, oxides of nitrogen and sulfur, and hydrocarbons can be evident on facial skin deterioration. Anti-pollution skin care is among the latest beauty trend that is on the rise. Global anti-pollution skincare products market value was nearly US$8 billion in 2020, and will expand to US$10 billion by 2026 at a CAGR of 3.8% [5]. Among the many ingredients driving anti-pollution beauty include charcoal or activated charcoal, vitamins E, sea salt minerals, and plant extracts [6]. Up to 76% of local respondents were willing to try and purchase locally produced charcoal-based personal care products.

The term biocarbon is loosely referred to porous, carbon-rich bio-charcoal or carbonized biomass material generated through thermal conversion of biomass or biological residues [7, 8]. Biomass sourcing, its subsequent preparation, and material modification will depend upon application purpose. Most charcoal or activated charcoal used in existing personal care products such as maskers, face wash, and shampoos are of bamboo-origin sourced from abroad. Many of these formulations are also water-based. In the context of this study, the biomass is sourced from coconut shells (hard portion) and dry leaves (soft portion) of *Macaranga gigantea* [9] which was then subjected to carbonization, activation, and surface modification. The biocarbon mix encompasses of (i) carbonized and salt activated material, and (ii) iron oxide impregnated biocarbon composites. Iron oxides can enhance adsorption characteristic, and are regarded safe for use in cosmetics and personal care products as they are non-toxic and non-allergenic, and well tolerated by those with sensitive skin.

Cyclopentasiloxane (CPS) was opted as the crosslinker in the synthesis of the iron oxide impregnated biocarbon composite. Cyclopentasiloxane or decamethylcyclopentasiloxane (D5) is a commonly used silicone compound ingredient in skin and personal care products. It helps to improve formulation texture while providing protection to the skin from moisture loss, allergens, and bacteria [10]. The inclusion of this compound has been considered to be safe [11].

The surface modified new biocarbon composite mix (NBC) is expected to provide the multi-action care and cleansing function in personal care products. This harnesses charcoal's natural strength due to large surface area coupled to iron oxide modified surface properties that facilitates washing, scrubbing, and adsorption. Furthermore, it can help remove environmental pollutants from outdoor exposure that is lodged in the face pores. From economy point of view, transformation of conventional charcoal or biochar material into value-added biocarbon composites for inclusion in high margin products such as personal care and cosmetics will be positive for local industry players.

This paper describes the preparation of NBC, followed by optimization of makeup foundation (MF) removal factors (adsorbent dosage, adsorbate concentration, particle size range, and contact time). Thereafter NBC was included in the formulation of a waterless charcoal-based masker. This work thus demonstrates the utilization of

agrobiomass residues converted to biocarbon composites as potential high value-added product for use in the formulation of waterless masker for skincare.

MATERIALS AND METHODS

Materials

Chemicals and reagents used included the following: hydrochloric acid, HCl (12 M), ammonium hydroxide, NH_4OH (0.7 M), sodium chloride (NaCl), iron (III) chloride hexahydrate ($FeCl_3.6H_2O$), iron (II) sulphate heptahydrate ($FeSO_4.7H_2O$), cyclopentasiloxane ($C_{10}H_{30}O_5Si_5$), caprylic triglyceride ($C_{55}H_{112}O_{11}$), shea butter, mango butter, Olivem 1000, beeswax, cetyl alcohol, rhassoul clay, sodium cocoyl isethionate (SCI), spa fine salt, rose extract, and distilled water. A well-known commercial makeup foundation, Focallure SKIN Evolution was chosen as the adsorbate [12]. Stock solution (100-500 mg/L) of the makeup foundation (MF) was made by dissolving it in caprylic triglyceride. The makeup foundation displayed maximum absorption at 499 nm (Spectrophotometer; Genesys 20). A commercial activated charcoal (CAC; Friendemann Schmidt Chemicals) and skin care product (CF; Freeman, detoxifying mud mask containing charcoal plus black sugar) was also included in this study.

Biomass Sourcing and Biocarbon Preparation

The fallen dry leaves of *M. gigantea* were collected on campus, and along the road side. The dry leaves were washed and cleaned from impurities, oven dried overnight, ground into fine powder, before sieved to ≤ 150 μm particle size range (Auto sieve shaker, Model: A060-01) and tagged as MLP. The waste coconut shells (CS) were collected from local coconut milk seller. Carbonization of the agrobiomass residues were achieved through top lit up-draft (TLUD) method by use of modified carbonization drum [13]. The carbonized CS was then crushed into powder form.

Biocarbon activation: The carbonized material was soaked in NaCl (30% w/v) for 24 h, at a ratio of 1:3.5, and heat treated at 500ºC (heating rate, 5 ºC/min) for 1 h (Muffle furnace; Carbolite ELF 11/6B). The activated biocarbon (ABC) was stored in an air-tight container.

Biocarbon composite preparation: A chemical coprecipitation method as described previously was followed with slight modification [13]. NH_4OH as a reducing agent was added dropwise to an aqueous solution made by mixing hydrated iron (III) chloride (1 mM) and hydrated iron (II) sulphate (0.5 mM) in a 2:1 molar ratio under continuous stirring (pH raised to 10-10.5). Activated biocarbon (ABC; 3% w/v) was added to the solution at 80 ºC-85 ºC, followed by cyclopentasiloxane (CPS) addition (1% - 2% v/v), and agitated (250 rpm) for 1-2 h. The mixture was then transferred to a sonicator bath (Daihan WUC-D22H) for another hour. The resulting modified new biocarbon composite (NBC) was filter-washed (vacuum pump; VP 260) repeatedly with water and ethanol until pH ~7, oven dried (80 ºC), and sieved accordingly to four particle size range groups, μm (N: 150 < x ≤ 300; O: 75 < x ≤ 150; P: 45 < x ≤ 75; and Q: ≤ 45). The biocarbon composite was examined through scanning electron microscopy (SEM) equipped with energy dispersive spectroscopy analyzer (EDS) (JEOL Model JSM IT100) with an acquisition time of 40 s and accelerating voltage of 15 kV. X-Ray diffraction (XRD) analysis (Cu Kα; λ = 1.5406 Å) was done with Bruker AXS D2 Phaser (Germany) diffractometer. Scan rate was 0.01 º/s, in the 10º-90º angle range.

Experimental Design

The optimized Box-Behnken experimental design for MF removal is presented in Table 1. A total of 24 runs were generated covering the given factors (A: dosage, B: concentration, C: particle size, and D: contact time) at three levels (-1, 0, 1). All runs were carried out at ambient room temperature (28 ºC ± 2 ºC).

TABLE 1. Experimental runs and factors for MF removal.

Run #	Experimental factor				Coded variable			
	Dosage (g) A	Concentration (mg/L) B	Particle size (µm)* C	Contact time (min) D	A	B	C	D
1	0.050	300.00	142.50	15.00	1	0	0	-1
2	0.005	300.00	142.50	60.00	-1	0	0	1
3	0.028	100.00	142.50	60.00	0	-1	0	1
4	0.050	500.00	142.50	37.50	1	1	0	0
5	0.028	300.00	142.50	37.50	0	0	0	0
6	0.028	500.00	142.50	60.00	0	1	0	1
7	0.028	100.00	60.00	37.50	0	-1	-1	0
8	0.050	300.00	225.00	37.50	1	0	1	0
9	0.028	300.00	142.50	37.50	0	0	0	0
10	0.028	300.00	142.50	37.50	0	0	0	0
11	0.028	100.00	225.00	37.50	0	-1	1	0
12	0.028	500.00	225.00	37.50	0	1	1	1
13	0.050	300.00	142.50	60.00	1	0	0	1
14	0.028	300.00	60.00	15.00	0	0	-1	-1
15	0.028	300.00	60.00	60.00	0	0	-1	1
16	0.005	300.00	225.00	37.50	-1	0	1	0
17	0.028	100.00	142.50	15.00	0	-1	0	-1
18	0.028	500.00	142.50	15.00	0	1	0	-1
19	0.005	500.00	142.50	37.50	-1	1	0	0
20	0.050	100.00	142.50	37.50	1	-1	0	0
21	0.050	300.00	60.00	37.50	1	0	-1	0
22	0.028	300.00	142.50	37.50	0	0	0	0
23	0.028	300.00	225.00	15.00	0	0	1	-1
24	0.028	300.00	142.50	37.50	0	0	0	0

Note: particle size range representation: 60 µm (-1: 45 < x ≤ 75); 142.5 µm, (0: 75 < x ≤ 150); 225 µm, (1: 150 < x ≤ 300).

Adsorption Experiment

Makeup foundation (MF) was prepared based upon the required concentration (100, 300, 500 mg/L) and the initial concentration (C_e, mg/L) was noted. A predefined amount of NBC and CAC (0.005, 0.028, and 0.05 g) was equilibrated with 5-10 mL of MF solution. The mixtures were placed in orbital shaker (Smith) for a determined period of time (15.00, 37.50 or 60.00 min) and agitated at 150 rpm. The residual concentration of MF solution at equilibrium was analyzed by UV-vis spectrophotometer (standard curve: $y = 0.0019x$, $R^2 = 0.9996$). The percentage removal of MF by NBC (MFR%) was calculated as: $(C_o - C_e)/C_o \times 100\%$; where C_o (mg/L) and C_e (mg/L) are the initial concentration, and residual concentration of MF at equilibrium, respectively. Variations in the functional groups of NBC before and after MF adsorption was investigated by Fourier transform infrared spectroscopy (FTIR; Thermo Scientific Nicolet iN10 Infrared Microscope & iZ10 FTIR module).

Kinetic Study

Kinetic study for MF removal by NBC was carried out at optimized parameter conditions as determined from the adsorption experiment. The contact time was varied from 5, 10, 15, 20 to 25 min. The adsorption capacity, q_e (mg/g) was calculated (Eq. 1); where w (g) is the amount of NBC, and V (L) is the volume of the solution. The kinetics of MF removal was investigated by using pseudo first-order (Eq. 2), pseudo second-order (Eq. 3) and intra-particle diffusion models (Eq. 4) [14, 15, 16]; where q_e and q_t are the adsorption capacity (mg/g) of NBC at equilibrium and at time, t, respectively. Meanwhile, k_1(min/1) is the first-order adsorption rate constant and k_2 (g/mg min) is the second-order adsorption rate constant. Based on Eq. (4), k_3 (mg/g. $min^{1/2}$) is the rate constant for intra-particle diffusion, and C (mg/g) is the constant that is determined by the thickness of the boundary layer. The larger the value of C, the greater the thickness of the boundary layer. The value of rate constant for pseudo first-order, pseudo second-

order and intra-particle diffusion can be determined by plotting log ($q_t - q_e$), t/q_t and q_t against t, t and $t^{1/2}$, respectively. The models will be selected based on linearity and goodness of correlation coefficient.

$$q_e = \frac{C_o - C_e}{w} \times V \quad (1)$$

$$\log(q_e - q_t) = \log(q_e) - \frac{k_1 t}{2.303} \quad (2)$$

$$\frac{t}{q_t} = \frac{1}{k_2 q_e^2} + \frac{t}{q_e} \quad (3)$$

$$qt = k_3 t^{1/2} + C \quad (4)$$

Cleansing Test

Rubbing test: The effectiveness of NBC in removing MF was evaluated by adopting a method described by Davies et al. and Walters et al. [17, 18]. Adsorbent suspension was created by mixing 0.1 g of NBC with 100 mL of distilled water. The test was also repeated by using ~ 2 g of the newly prepared masker formulation. The back of the hand area was cleaned prior to the rubbing test. This was to remove impurities or any contaminants from the skin surface. Makeup foundation was spread on the back of the hand for a length of 3 cm and the coated foundation was left to dry for about 2 min. NBC suspension was dropped dropwise onto the skin. Makeup stain was rubbed with NBC suspension. The rubbing process was conducted by using only two fingers. The number of rubbing and the volume of NBC suspension at the disappearance of the MF from skin was recorded as a measure of cleansing effectiveness of NBC. The test was repeated thrice. The removal of MF by NBC was compared with removal by using only water.

Color removal: The removal of MF color by NBC was investigated using a method modified from Kishina et al. [19]. The color removed after rubbing is evaluated based on color intensity difference. One drop of MF was spread on a glass slide (2 cm in diameter) and left to dry for one day. An NBC suspension was prepared by mixing 0.5 g NBC with 50 mL of distilled water. The measurement of MF color before rubbing was examined using chroma meter (CR400 Konica Minolta). The glass slide with dried MF film was lightly rubbed for 10 times under running NBC suspension. After the 10th time, the film was lightly pressed with tissue paper and observed for any MF coming off. The color difference of MF on the glass slide was analyzed by using CIE L*a*b* coordinates [20]. The total color difference (ΔE*) was calculated as in Eq. (5) [20]; where L_1^*, a_1^* and b_1^* represent lightness, redness/greenness and yellowness/blueness of the sample before running under flowing NBC suspension, respectively. Meanwhile, L_2^*, a_2^* and b_2^* indicate the corresponding colour after the test been conducted.

$$\Delta E^* = \sqrt{(L_2^* - L_1^*)^2 + (a_2^* - a_1^*)^2 + (b_2^* - b_1^*)^2} \quad (5)$$

Masker Formulation

The base formulation was modified from Rayma [21]. A total of 12 sample formulations (S1-S12) were derived (Table 2). The masker preparation was divided into three phases (heated oil, powder, and cooling down). Beakers and spatulas were autoclaved (121 °C, 15 min) prior to use.

TABLE 2. Suggested formulation of masker.

	Samples											
Ingredients, %	S1	S2	S3	S4	S5	S6	S7	S8	S9	S10	S11	S12
Olivem1000	15	10	5	2	2	3	3	3	3	3	3	3
Beeswax	-	-	-	-	-	-	-	-	-	1	-	2
Cetyl alcohol	2	12	12	12	12	12	12	12	12	12	12	12
Shea butter	20	10	10	10	-	-	-	-	-	-	-	-
Mango butter	-	-	-	-	10	10	10	10	10	12	10	10
Glycerine	-	-	-	-	-	-	-	-	-	-	3	-
Grapeseed oil	42	35	33	33	33	32	32	30	30	24.5	24.5	24.5
NBC	1	1	1	1	1	1	1	1	1	1.5	1.5	1.5
Rhassoul clay	11	22	22	25	25	24	24	24	24	25	25	25
SCI	5	5	12	12	12	12	12	13	13	14	14	15
Spa fine salt	3	3	3	3	3	3	3	3	3	3	3	3
Rose extract	1	2	2	2	2	3	3	4	4	4	4	4

First, the oil phase ingredients (Olivem 1000, beeswax, cetyl alcohol, shea butter/mango butter, glycerine, and grapeseed oil) were weighed, heated, and melted in a beaker using water bath (70℃ - 85℃; 20-30 min). Sequence of addition followed the decreasing order of their melting point. This was followed by the mixing of powder phase ingredients (rhassoul clay, SCI, spa fine salt, NBC). The mixture was stirred well until no clumps were visible. Then an ice bath was prepared by filling in ice cubes and cold water in a bowl. The mixture was placed in the ice bath and stirred until it gained viscosity. Finally, the cooling down phase ingredient (rose extract) was added, and stirred until a uniformed masker texture was observed. All the 12 formulations were left to stand for 48 h before any tests were carried out.

Characterizing Masker Formulation

In order to determine the stability of the formulation mix, the samples were subjected to preliminary organoleptic tests consisting of pH, colour, odor, touch and spreadability, and oily layer formation [22]. The outcome of each parameter observation was categorized numerically as either (1) most acceptable, (2) less acceptable, or (3) not acceptable. This was followed by further tests as described hereon [22].

Storage stability test: The evaluation was conducted at three conditions. The best masker formulation was stored in a refrigerator (cold temperature; 4 ℃ ± 1.0 ℃), left at room temperature (26 ℃ ± 2.0 ℃), and put in an oven (hot temperature; 40 ℃ ± 2.0 ℃) for 14 d. Any signs of alterations in color, odor or texture were noted. Microbe screening: The prepared masker sample was streaked onto nutrient agar (NA) plate and left at room temperature for 48 h. Light exposure test: The test was done by placing the best masker formulation in two situations. One exposed to normal daily sunlight and UV light. The other set was covered with aluminum foil. Any signs of alterations in color, odor or texture were observed. Texture profile analysis (TPA): The formulated masker texture was tested for hardness, resilience, and cohesiveness with a Texture Profile Analyzer (CT3 Texture Analyzer, Brookfield Engineering, USA) with cylinder probes (TA-DEC, probe: TA17 and TA18). Test type was set to TPA, target distance: 5-10 cm, test and return speed: 10 mm/s, trigger load of 5 g. The presence of water in the selected formulations were investigated by using Fourier transform infrared spectroscopy (FTIR; Thermo Scientific Nicolet iN10 Infrared Microscope & iZ10 FTIR module).

RESULTS AND DISCUSSION

Optimization of Adsorption Parameters

The experimental and predicted MF removal (MFR%) responses for the 24 runs is presented in Table 3. The highest MF removal of 88.07% was attained at an adsorbent dosage of 0.028 g, adsorbate concentration of 300 mg/L, NBC particle size of 225.00 μm (N: $150 < x \leq 300$ range) and with 15 min contact time (run #23). The lowest removal percentage was 40.19%, which was at a higher MF concentration (500 mg/L), and smaller adsorbent dosage (0.005 g).

TABLE 3. Experimental MF removal (MFR%) responses.

Run	Experimental MF removal (MFR%)
1	86.92
2	66.73
3	58.94
4	81.78
5	85.18
6	87.42
7	63.73
8	86.64
9	85.18
10	85.18
11	67.57
12	87.13
13	86.40
14	81.75
15	73.90
16	77.84
17	80.00
18	71.44
19	40.19
20	55.91
21	82.71
22	85.18
23	**88.07**
24	85.18

The obtained data was fitted to various process descriptive models. Over the many comparative models available, quadratic model was selected as the best (Table 4). The adjusted R^2 value of quadratic model is the highest (R^2 = 0.9730) compared to other models and has the lowest standard deviation value (2.05). The predicted R^2 value of 0.8175 is less than the adjusted R^2 only by 0.155 difference, is highly desirable.

The analysis of variance (ANOVA) of the quadratic model is presented in Table 5. The F-value for the quadratic model is 60.25 and Prob > F value is less than 0.05. High F-value implies that the model is significant. The coded responses represented the following, A: dosage of adsorbent; B: concentration of MF solution; C: particle size of adsorbent; D: contact time. The value of Prob > F that is less than 0.05 indicates significant model terms, while those higher than 0.05 are insignificant. Thus, the fitted quadratic model is deemed significant.

Factor wise, only two out of the four selected factors were significant towards MF removal, i.e., dosage and particle size, whereas contact time was the most insignificant with Prob > F value of 0.9100. Based on their F-value, adsorbent dosage (A) had the highest reading, indicating that it had the most influence in makeup removal, followed by adsorbent particle size (C), adsorbate concentration (B), and contact time (D). In terms of square, only dual interaction of adsorbent dosage and dual interaction of makeup solution concentration were significant with F-values of 101.55 and 258.82, respectively. Dual interaction of particle size and contact time were insignificant with F-values of 1.37 and 9.51. Observing the interaction terms, only the interaction effect between dosage and concentration, and between concentration and contact time were significant to the responses with F-values of 48.85 and 81.85, respectively. The interaction between dosage and contact time had the least effect and was the most insignificant with Prob > F value of 0.6519, and the lowest F-value (0.22). The sum of square for lack of fit value (37.72) was also lower compared to the sum of squares of the model (3534.58). Overall, the model was sufficient to ascertain experimental responses of MF removal by NBC. Subsequently, the MF removal (%) model equation was generated (Eq. 6).

$$\text{MF removal } \% = 85.18 + 10.93A + 3.89B + 8.41C + 0.089D - 11.76A^2 - 14.61B^2 - 1.13C^2 + 2.88D^2 + 9.89AB - 6.98AC - 0.66AD + 6.12BC + 9.26BD + 5.07CD \quad (6)$$

TABLE 4. Model summary.

Model	Standard deviation	R-squared	Adjusted R-squared	Predicted R-squared
Linear	11.87	0.2503	0.0925	-0.26927
2FI	10.37	0.6086	0.3076	-0.6249
Quadratic	2.05	0.9894	0.9730	0.8175

TABLE 5. Analysis of variance (ANOVA) for response surface quadratic model.

Source	Coefficient	Sum of squares (SS)	Mean square (MS)	F-value	Prob > F	Comment
Model	85.18	3534.58	252.47	60.25	**< 0.0001**	Significant
A	10.93	523.84	523.84	125.00	**< 0.0001**	Significant
B	3.89	117.66	117.66	28.08	0.0005	
C	8.41	405.22	405.22	96.70	**< 0.0001**	Significant
D	0.089	0.057	0.057	0.014	0.9100	
A^2	-11.76	425.54	425.54	101.55	**< 0.0001**	Significant
B^2	-14.61	1084.64	1084.64	258.82	**< 0.0001**	Significant
C^2	-1.13	5.76	5.76	1.37	0.2713	
D^2	2.88	39.85	39.85	9.51	0.0131	
AB	9.89	204.72	204.72	48.85	**< 0.0001**	Significant
AC	-6.98	101.57	101.57	24.24	0.0008	
AD	-0.66	0.91	0.91	0.22	0.6519	
BC	6.12	89.20	89.20	21.29	0.0013	
BD	9.26	342.99	342.99	81.85	**< 0.0001**	Significant
CD	5.07	60.23	60.23	14.37	0.0043	
Residual		37.72	4.19			
Lack of fit		37.72	7.54			
Pure Error		0.000	0.000			
Cor Total		3572.29				

A: dosage of adsorbent; B: concentration of MF solution; C: adsorbent particle size; D: contact time.

The coded responses represented: A: dosage of adsorbent; B: concentration of MF solution; C: particle size of adsorbent; D: contact time. The positive and negative signs in front of the terms indicate synergistic or antagonistic effects, respectively. The difference between experimental MF removal percentage and predicted MF removal percentage is shown in Figure 1. As seen from Table 3 and Figure 1, the MF removal difference between predicted and experimental responses were low, in the range of -2.1% to 3.45%. This indicated the reliability of the observed occurrence of MF removal by NBC.

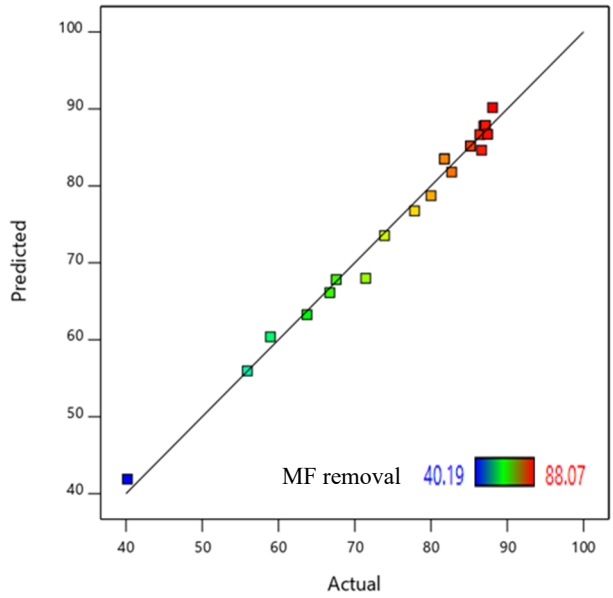

FIGURE 1. Plot showing the difference between predicted and actual MF removal percentage responses.

Effect of Variables and Their Interaction

The response surface plot of the respective independent variables (A: NBC dosage, B: MF concentration, C: particle size of NBC, and D: contact time) are given in Figure 2 (I-VI). The plot illustrates the interactions between the variables towards MF removal. The color shading from blue to red indicate MF removal (%) from 40.19% to 88.07%, respectively. Fig. 2 (I) shows that at higher MF concentration (200-500 mg/L), the % removal increased as the adsorbent dosage also increased (0.028-0.050 g). Lower adsorbent dosage (0.005-0.016 g) leads to lower MF removal (%). Increased quantity of NBC provides more readily available binding sites for adsorption. Fig. (II) depicts increase in MF removal (%) as adsorbent dosage and particle size increased. It can be seen from the contour plot that the MF removal was more efficient at higher amount of adsorbent (> 0.028 g) and larger particle size (> 60 µm). Low dosage of adsorbent of smaller particle sizes resulted in reduced MF removal (%). Observation showed that the larger particle size (225.00 µm) in the 150-300 µm range had greater influence on MF removal regardless of adsorbent dosage used. In Fig. 2 (III), it is also shown that MF removal increased with the increase in concentration of adsorbate (200-500 mg/L) and adsorbent particle size (> 150 µm). At higher concentration of MF, the % removal was more distinct as particle size increased. If smaller particle size were used at any adsorbate concentration, there is a reduction in MFR%. These findings are in agreement with a research by [23], where the efficiency to adsorb Pb(II) increased as the particle size (0.3-2.0 mm) and adsorbate concentrations (50-130 mg/L) were increased. The particle size of NBC in the range of 150-300 µm provided the better surface contact for optimum MF removal. From Fig. 2 (IV), it can be seen that MF removal was independent of contact time, as MF removal increased with dosage increase at any given time. At a fixed amount of dosage, MFR% was similar (55%) over 15 min and 60 min. Initial adsorption was rapid due to the large unoccupied binding sites, surface area, and affinity of NBC towards the adsorbate. This will shorten the time to attain equilibrium. The effect of MF concentration and contact time were more significant (as also seen from F-value in Table 5) towards MF removal. As seen in Fig. 2 (V), MF removal increased with the increase in concentration and contact time. For shorter contact time, MFR% was lower as the MF concentration was increased. Sufficient time is needed to allow greater surface contact for adsorption to occur. MF removal was better when contact time was prolonged (15-60 min). This permits the formation of MF layer on the surface with NBC throughout the process. The interaction of particle size and contact time effect is shown in Fig. 2 (VI). MF removal decreased as concentration increased and contact time shortened. The F-value for these interactions was also lower (Table 5).

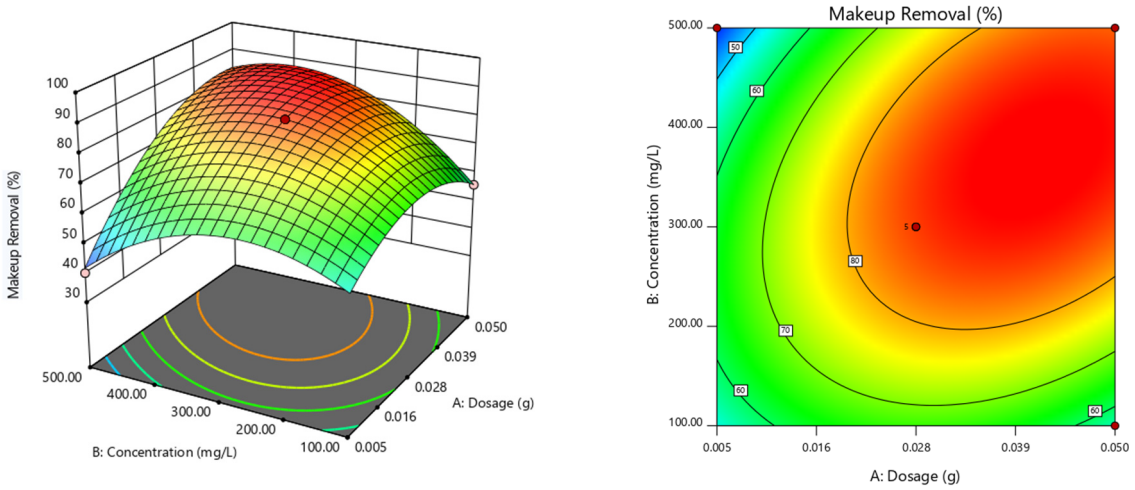

(I)

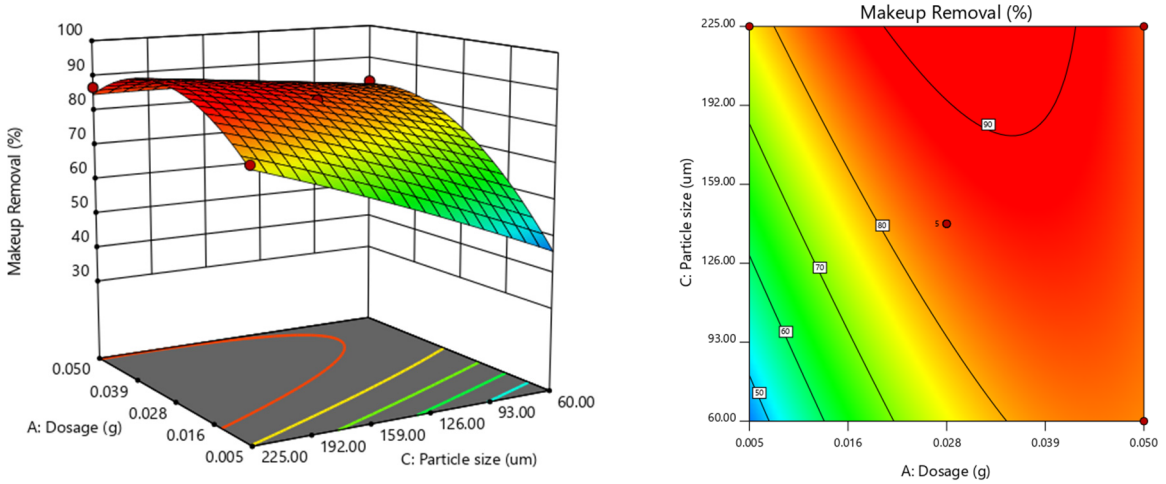

(II)

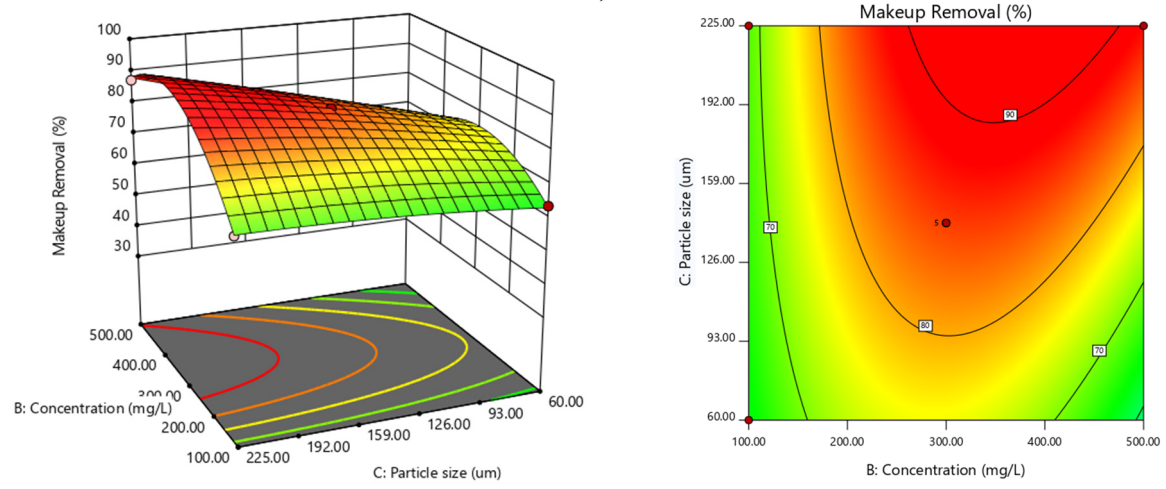

(III)

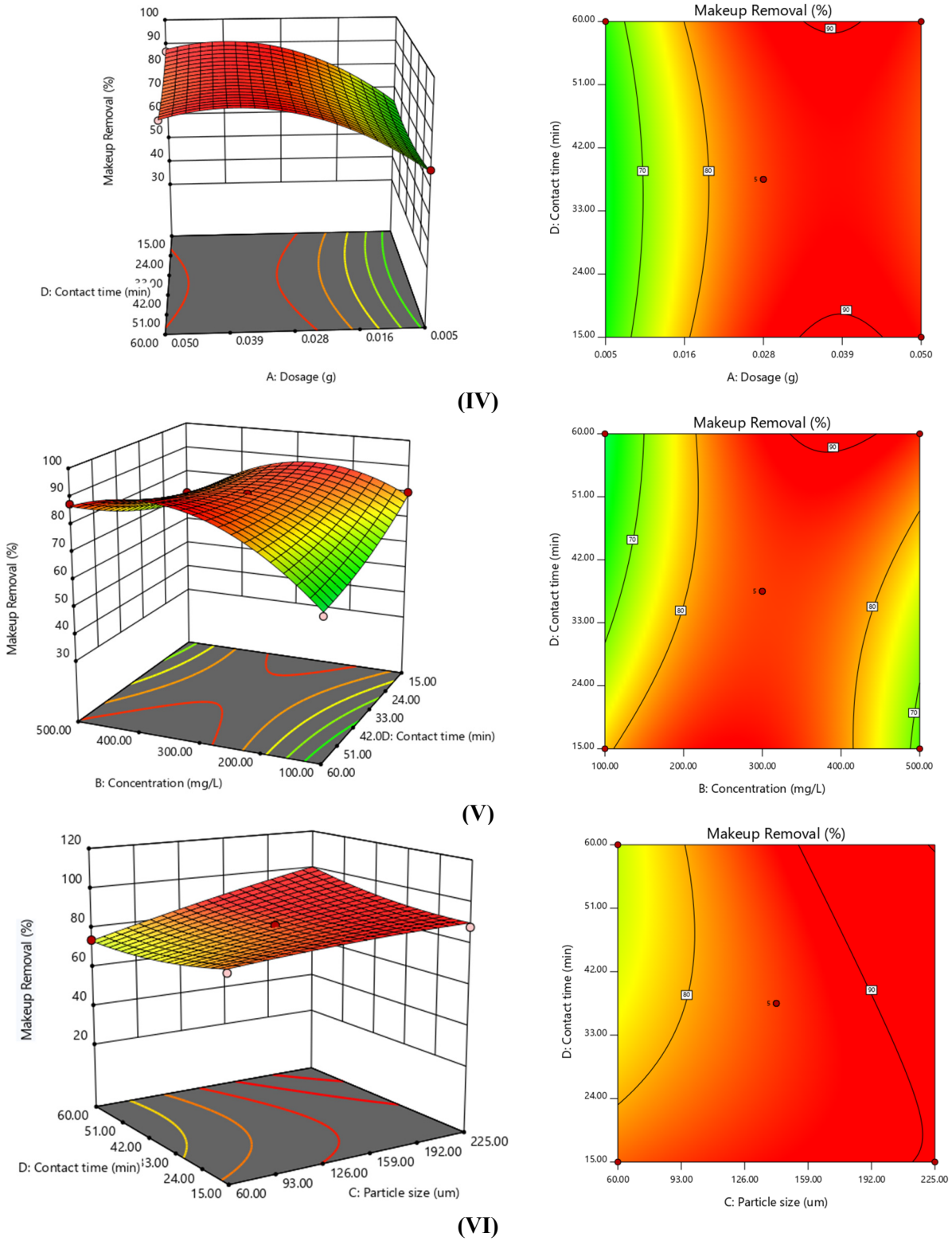

FIGURE 2. Response diagram showing the interactions of (I) adsorbent dosage (A) and adsorbate concentration (B); (II) adsorbent dosage (A) and particle size (C); (III) adsorbate concentration (B) and particle size (C); (IV), adsorbent dosage (A) and contact time (D); (V) adsorbate concentration (B) and contact time (D), and (VI) adsorbent particle size (C) and contact time (D), towards MF removal.

Adsorption Kinetics

Adsorption kinetics is a significant factor in MF removal. As such the following models (i.e., pseudo first-order, pseudo second-order, and intra-particle diffusion) were applied to understand the process kinetics. The linearized plots for the respective models are presented in Figure 3. The rate constant value for pseudo first-order (k_1), pseudo second-order (k_2) and intra-particle diffusion (k_3) were obtained from the slopes and intercepts of the linear plots [24]. Additional relevant kinetic parameters are listed in Table 6. The highest correlation coefficient value ($R^2 = 0.9993$) was obtained with pseudo second-order model as opposed to the other models. The rate of occupation of active sites is proportional to the square of the number of the unadsorbed sites on NBC. The model described and fitted well with the experimental findings. The adsorption capacity of NBC at equilibrium (q_e) of 27.32 mg/g calculated with the pseudo second-order model was near to the experimental adsorption capacity at equilibrium which was 26.48 mg/g. From the experimental data, the rate constant, k_2 of pseudo second-order model was calculated to be 0.04 g/mg min. The model presumes that adsorption is not occurring exclusively onto a single site and that the process is governed by chemical reaction rate [16, 24]. Therefore, the rate-limiting step of MF adsorption process onto NBC is controlled and proceeds by surface chemisorption. Chemisorption involves valence forces through the exchange or sharing of electron between NBC which is the adsorbent and the MF solution which is the adsorbate. Most probably involving C=O, C=N, C=ONH, O-H, and NH_2 groups, and possible complexation between Fe-O-C. Based on Fig. 3 (c), as the line did not pass through the origin, this meant that intra-particle diffusion model was not the only rate determining factor. This suggests some level of boundary layer control and other kinetic models that may control the rate of adsorption, all of which may be operating simultaneously.

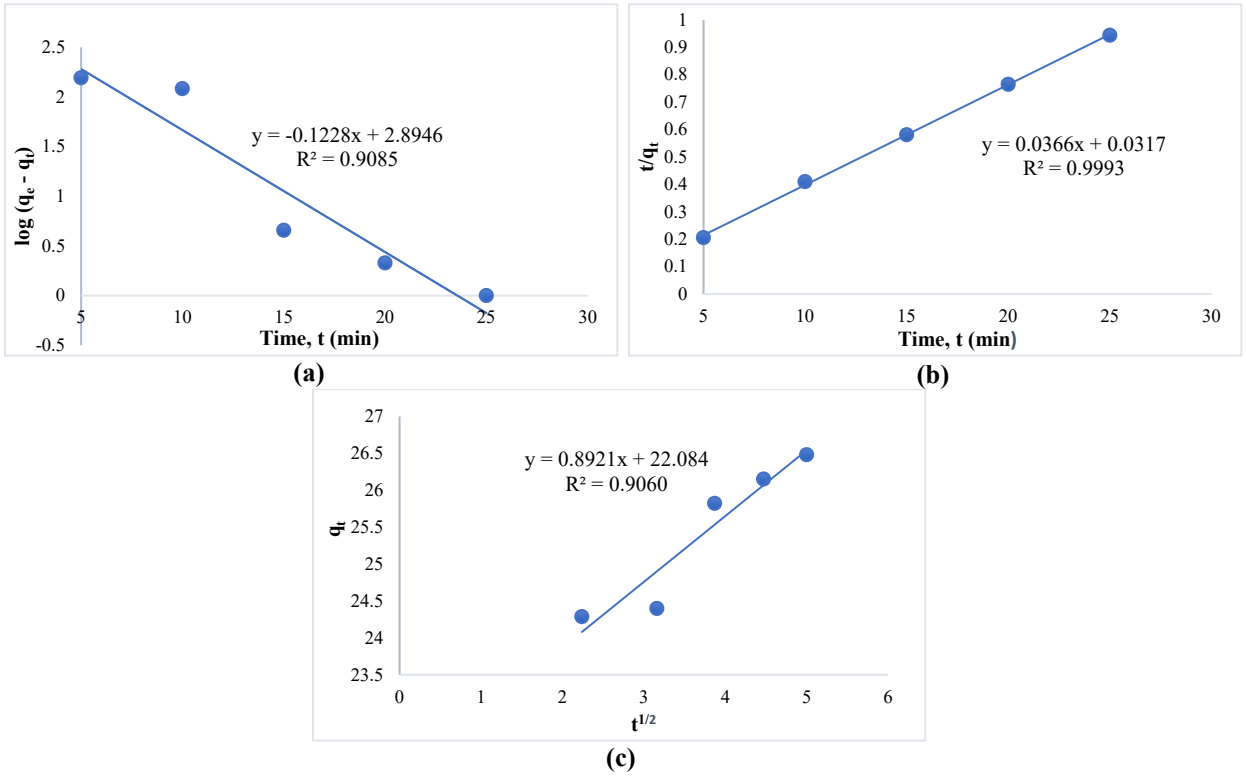

FIGURE 3. Kinetic model plots, (a) pseudo first-order, (b) pseudo second-order, and (c) intra-particle diffusion.

TABLE 6. Kinetic parameters.

Model	Parameter	Value
Pseudo-first order	k_1 (min/1)	0.28
	q_e (mg/g)	1.06
	R^2	0.9085
Pseudo-second order	k_2 (g/mg min)	0.04
	q_e (mg/g)	27.32
	R^2	0.9993
Intra-particle diffusion	K_3 (mg/g $min^{1/2}$)	0.8921
	C (mg/g)	22.08
	R^2	0.9060

Characterization of NBC

FTIR analysis: The understanding of NBC's adsorption ability in removing MF was inspected through FTIR scans. Figure 4 illustrates peak presence before and after NBC was subjected to MF adsorption. Apart from the usual alkyl, carboxyl, amide, hydroxyl groups, represented by C-C, C-H, C=C, C=N, C≡N, N=N, C=O, and O-H among others, new peaks were captured in spent NBC samples (after MF adsorption). The absorption peaks between 1090 cm^{-1} and 500 cm^{-1} pointed to the presence of C–O stretching and metal–oxygen (M–O) bands due to the interaction of iron and oxygen [25, 26]. Peak shifts were observed as with a peak at 2287.68 cm^{-1} which shifted to 2329.98 cm^{-1} after adsorption. This can be due to C=N stretching vibration of alkyl group which may be aryl nitrite. The movement of another peak from 2087.64 cm^{-1} to 2113.55 cm^{-1} showed probable participation of ketenes and Si-H stretching vibration. The sharp peak at 1736.66 cm^{-1} corresponds to C=O and C=C stretching vibration of ketone group. Addition of two other peaks in NBC after adsorption at 2919.91 cm^{-1} and 2851.63 cm^{-1} were attributed to methyl group stretching vibration (CH_3, CH_2). This observation suggests that the additional functional groups arise from the multi-constituents of MF being adsorbed by NBC. Based on the peak ranges, these functional groups are related to compounds of trans olefins, aliphatic acetate esters and aliphatic ethers [25]. This supports the suggested chemisorption interaction between NBC and MF constituents during adsorption process.

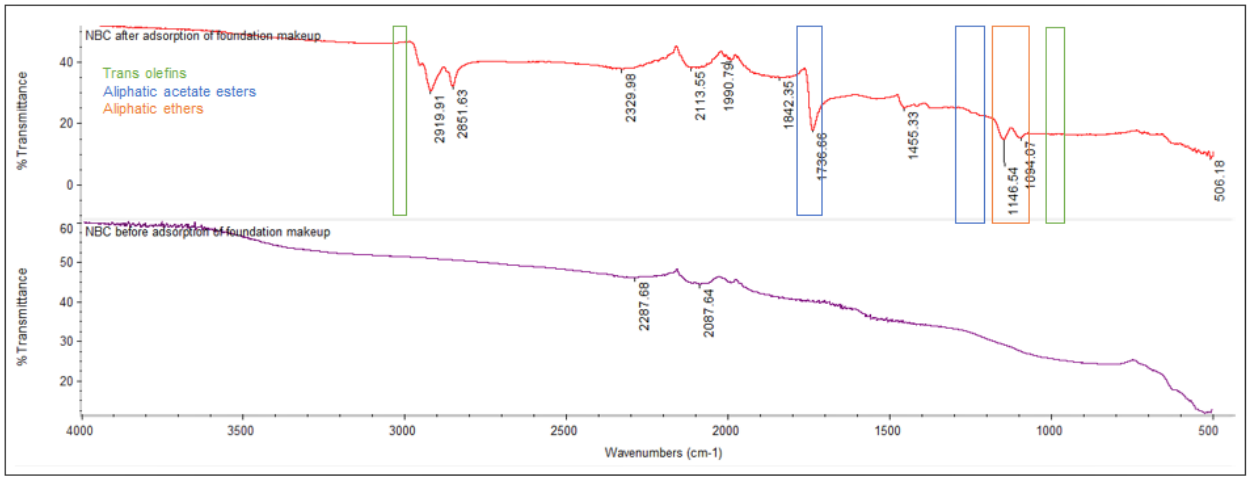

FIGURE 4. FTIR spectra of NBC before and after rubbing of MF.

SEM examination: As observed from Figure 5 (a) and 5 (b), presence of micropores were evident on the heterogenous biocarbon composite surface. However, most are surrounded or covered by iron oxide deposits impregnated onto the biocarbon. Impregnation of the biocarbon with iron oxide particles can enhance adsorption capability. Elemental scanning (atomic, %) as seen in Figure 5 (c) revealed that the composite is made up of C (47.20%), O (33.31%), Fe (17.19%), and Si (1.80%). The presence of Si as detected in both FTIR and SEM-EDS originates from the cross-linking agent used, i.e., CPS ($C_{10}H_{30}O_5Si_5$). The SEM image resembles the observation noted

by [26] in the synthesis of magnetic activated carbon from palm kernel shells. The composition differed in terms of C (32.83%), O (45.48%), and had P (1.32%) due to the use of H_3PO_4. Iron content was close to NBC at 20.37%.

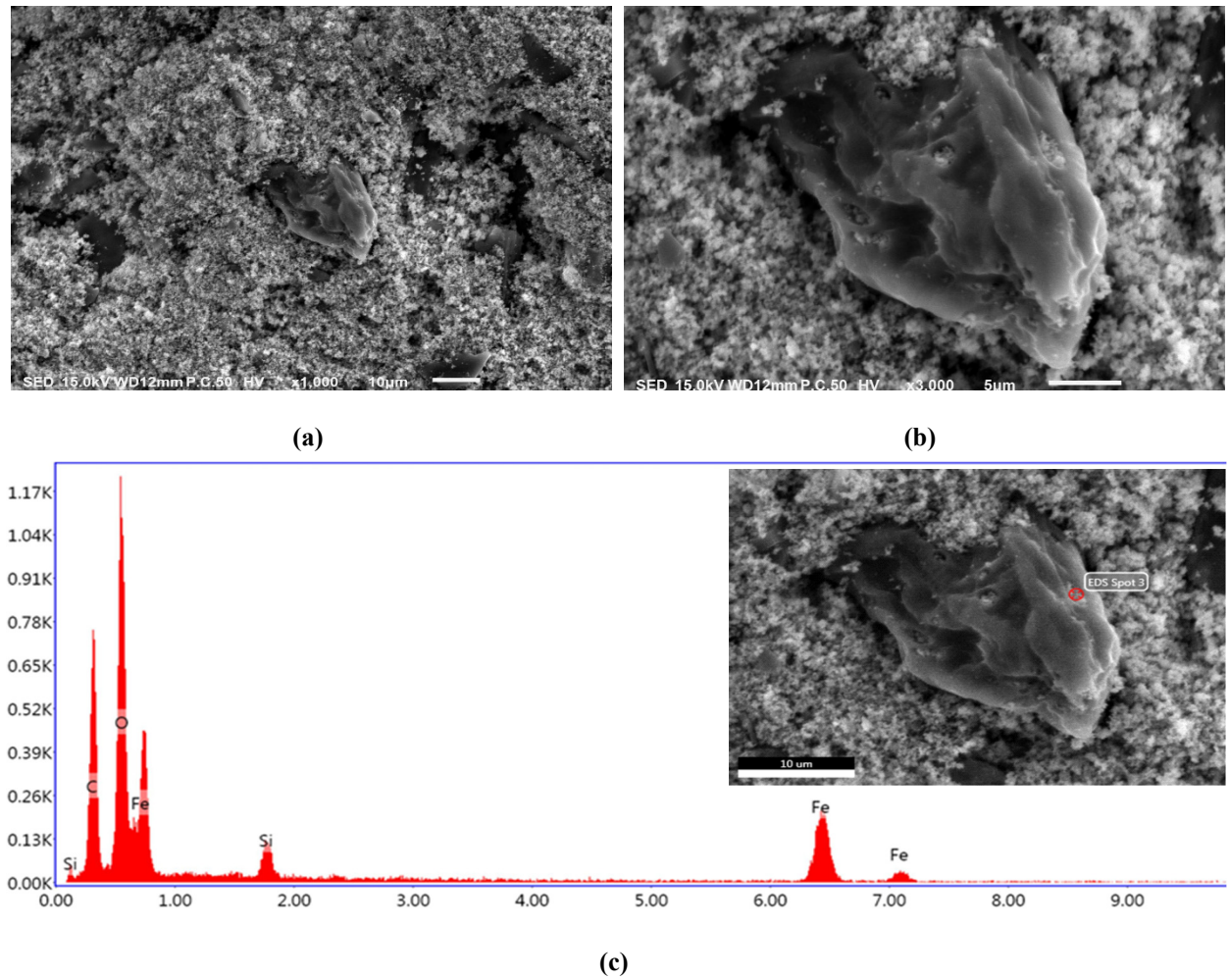

FIGURE 5. SEM imaging of NBC at different magnifications (a) x 1000, (b) x 3000, and (c) SEM-EDS spectrum of NBC.

XRD analysis: Figure 6 (a) showed intense sharp peaks in NBC denoting the microcrystalline phase of iron oxides. Three peaks at 2θ values of 30.16°, 35.54°, 57.30° were assigned to Fe_3O_4 (magnetite), and another three peaks at 43.10°, 53.56°, and 62.80° were attributed to γ-Fe_2O_3 (maghemite). Based from the literature [24, 26], the peaks corresponded to (220), (311), (400), (422), (511), and (440) cubic indices planes, respectively. The major diffraction peak at 35.54° (311), supported by the remaining minor peaks reflect the spinel structure of iron oxide to consist of only magnetite (Fe_3O_4) and maghemite (γ-Fe_2O_3), and not hematite (α-Fe_2O_3) or goethite [α-FeO(OH)] forms. Similar XRD patterns of magnetite and maghemite have been reported previously by [26] during the synthesis of magnetic palm kernel shell. The presence of iron oxides in the form of magnetite and maghemite suggested NBC to display magnetic properties. Magnetite possesses iron cations in two valence states, i.e., Fe^{3+} and Fe^{2+}. The synthesis of iron oxide impregnated biocarbon composite had been achieved. The stability of the composite was monitored by soaking NBC in water, agitated daily, and left to stand up to 30 days. No evidence of iron leaching was observed (Iron checker, Hanna HI 721). On the other hand, structure of CAC, Fig. 6 (b) was predominantly amorphous with broad peaks in the range of 2θ = 10°-30°.

The crystallite size of the iron oxides was estimated by using the Debye-Scherrer formula (Eq. 7) where d_{avg} is the average crystallite size (nm), K: Scherrer constant (0.94), λ is the incident x-ray wavelength (CuKα = 1.5406 Å), β is the line broadening, full width at half maximum (FWHM) in radians, and θ is the diffracted angle. The average

crystallite size for Fe_3O_4 (magnetite) distribution was 65.56 nm, and 96.61 nm for γ-Fe_2O_3 (maghemite). The biocarbon composite used was in the $150 < x \leq 300$ μm particle size range.

$$d_{avg} = \frac{K\lambda}{\beta \cos \theta} \tag{7}$$

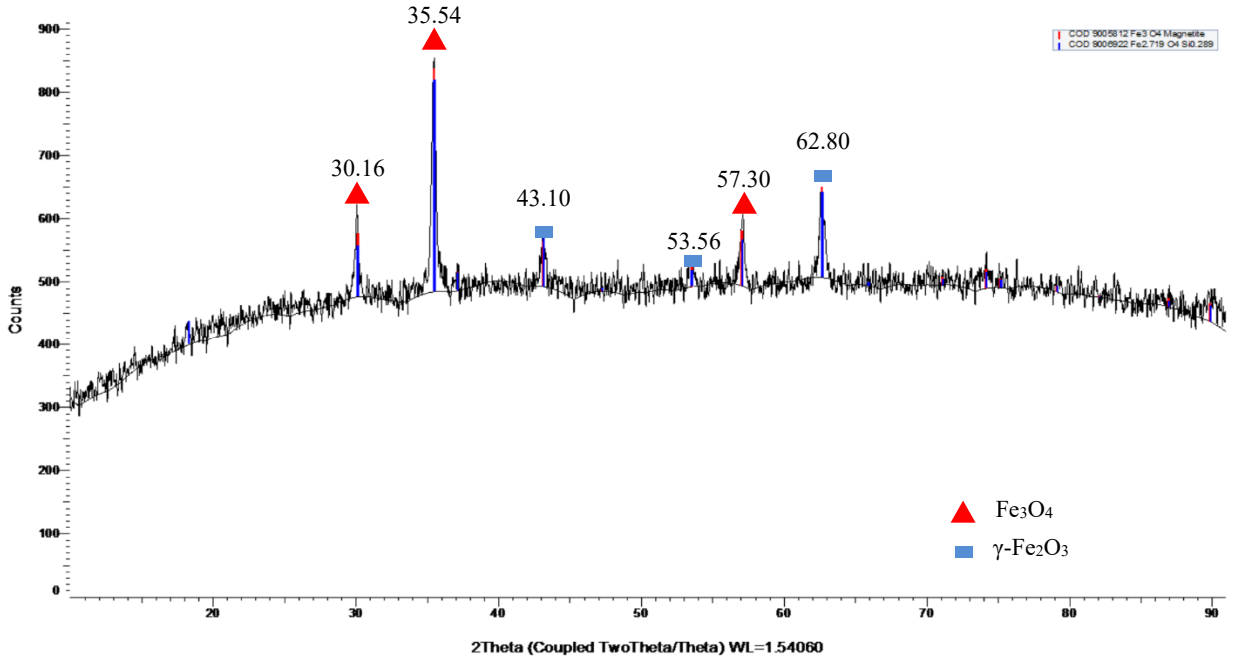

(a)

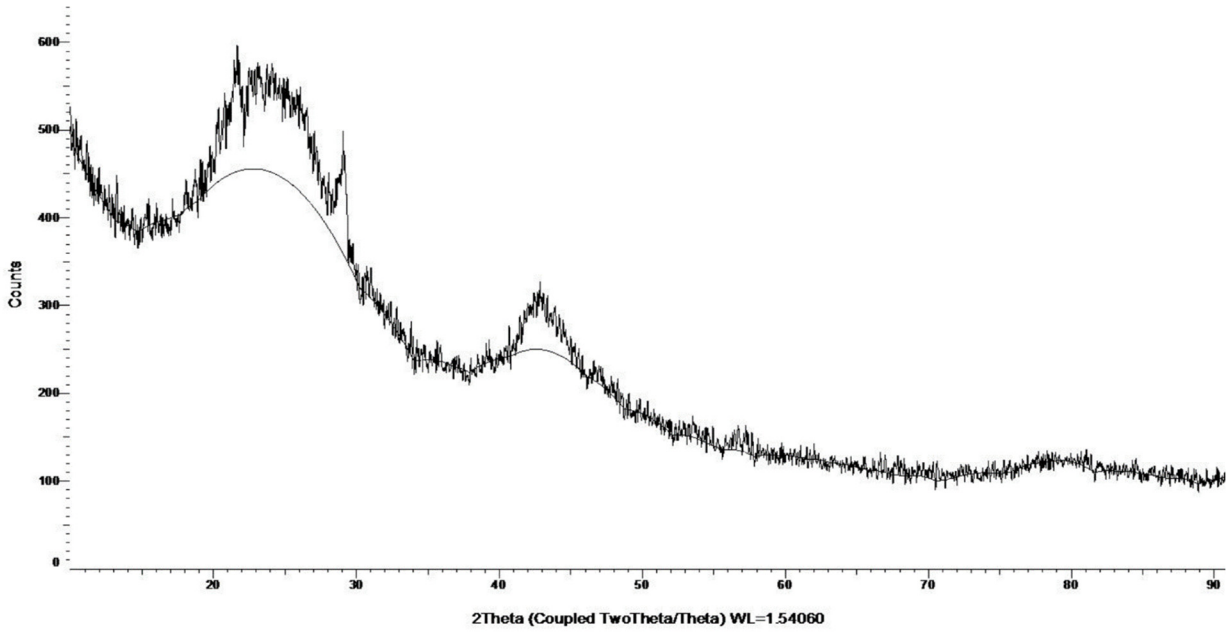

(b)

FIGURE 6. XRD spectra of (a) NBC and (b) CAC.

Ferromagnetic nanoparticles of iron oxides, i.e., maghemite (γ-Fe_2O_3) and magnetite (Fe_3O_4) have been widely used as effective sorption agent for numerous chemical compounds including antibiotics, heavy metals, and organic dyes [14, 24, 27, 28, 29]. The use of iron oxide nanoparticles in their free form is not preferred as γ-Fe_2O_3 tend to form aggregates due to high surface energy arising from strong van der Waals forces [14, 30]. This will decrease effective surface area and adsorption abilities. Hence, employing biocarbon as a platform to harbor the iron oxide particles can alleviate this issue. The biocarbon generated from agrowaste biomass can provide support to enhance stability of the iron oxide particles. The iron oxide loaded biocarbon can be infused in personal care products as many cosmetic products list iron oxides as their ingredients. Furthermore, iron oxide coated materials are reported to have antibacterial activity [4, 6].

Masker Formulation Outcome

Based on the capability of NBC in removing MF, NBC was opted for inclusion in the masker formulation. A total of 12 formulations were prepared. The use of shea butter in the initial formulations (S1-S4) resulted in oily mixtures which was less desirable. Hence, the latter formulations (S5-S12) utilized mango butter which gave a more appealing final mixture outcome. During mixing, attention must be given to ensure complete dissolving of SCI. This can be achieved by prior grinding and homogenization of the powder before adding into the mixture. The overall observation of the formulation outcome is listed in Table 7. Evaluation was made based on color, odor, touch and spreadability, presence of oily layer on top, and pH. A commercial charcoal-based product (CF; Freeman Detoxifying mud mask containing charcoal plus black sugar) was used as benchmark comparison. In terms of color, most acceptable color was in the tone of light to dark grey, followed by dark grey to black. Uneven color formation is not acceptable as it reflects poor blending and incompatibility of ingredient components. Almost all samples displayed acceptable color range except for S1, S3 and S7. Odor wise, S1 had a very unpleasant smell, followed by S3, S6, and S8. An important feature for any masker formulation would be its touch and spreadability characteristics. The texture must be pleasant to touch, feels even and full, non-oily or greasy, and easy to spread. Only the latter sample formulations, i.e., S9-S12 fulfilled these criteria. Among these 4 samples, only S10 (pH 7.3) was consistent throughout and did not show any formation of oily layer on top. Formation or presence of oily layer after 48 h may indicate unstable formulation, and poor blending-in of the ingredient's mixture. The pH value did not show any variations beyond 15% from the initial value. In preliminary cosmetic formulation studies, physical and physicochemical stability assessment are of importance as followed by [21]. Evaluation of the samples emphasized on formulation consistency observed through acceptability scale, covering aspects of color, odor, touch and spreadability, presence of oil layer, and pH. Hence, S10 was identified as the best sample formulation, and subjected to further tests.

TABLE 7. Overall observation of the prepared formulation samples.

	Evaluated parameters				
Formulation	**Color**	**Odor**	**Touch and spreadability**	**Presence of oily layer**	**pH Value**
S1	3	3	3	2	6.9 ± 0.20
S2	2	1	3	2	6.5 ± 0.11
S3	3	2	2	2	6.6 ± 0.30
S4	1	1	2	3	7.4 ± 0.06
S5	1	1	2	3	7.3 ± 0.06
S6	2	2	2	1	7.1 ± 1.09
S7	3	1	2	3	6.3 ± 0.26
S8	1	2	2	1	6.5 ± 0.00
S9	2	1	1	2	7.3 ± 0.00
S10	**1**	**1**	**1**	**1**	**7.3 ± 0.00**
S11	1	1	1	2	7.8 ± 0.06
S12	1	1	1	2	6.6 ± 0.30
CF	1	1	1	1	7.7 ± 0.00

Note: Observation outcome, **Color**: (1) most acceptable, (2) less acceptable, (3) not acceptable; **Odor**: (1) most acceptable, (2) less acceptable, (3) not acceptable; **Touch and spreadability**: (1) most acceptable - pleasant to touch, easy to spread, (2) less acceptable – a bit oily, easy to spread (3) not acceptable, unpleasant touch, oily, hard to spread; **Presence of oily layer**: (1) most acceptable – no oil layer, (2) less acceptable – slightly visible oil layer, (3) not acceptable – thick oil layer. For **pH**, the values presented are mean ± standard deviation (n=3).

Storage stability test: The chosen formulation mix (S10) was subjected to stability test by storing it at various conditions for 14 d (Table 8). In comparison to commercial masker product, S10 showed slight change in its texture at 4 °C and 40 °C. It is to be noted that, S10 is completely a raw formulation and has no added stabilizers or preservatives. Moreover, it is prepared in a research laboratory setting and not in a GMP facility as opposed to CF. Nevertheless, S10 remained stable with no significant change in color, odor, and pH.

TABLE 8. Observation outcome for storage stability test at varying temperatures.

Sample	Cold temperature (4 ± 1.0 °C)	Room temperature (26 ± 2.0 °C)	High temperature (40 ± 2.0 °C)
S10	SC	NC	SC
CF	NC	NC	NC

Note: NC-no change; SC-slight change; IC-intense change

Light exposure test: Table 9 shows that no significant changes were observed with both S10 and CF samples after exposure to UV and sunlight. This showed that the formulated sample was stable at all conditions. This is an important indicator that the formulation will be able to hold up throughout their shelf-life. No color alteration was observed, signifying good stability at varying conditions and compatibility of the formulation even without water. The masker mix also did not show any signs of over-drying throughout the test. The texture form of S10 was intact.

TABLE 9. Observation outcome for light exposure test at room temperature.

Parameters	S10		CF	
	Exposed	Not exposed	Exposed	Not exposed
Color	No change	No change	No change	No change
Odor	No change	No change	No change	No change
Texture	No change	No change	No change	No change

Microbe screening test: Nutrient agar (NA) was used as it can support the growth of many microbes. No visible change or microbial growth indication was seen after 24 h and 48 h. The absence of water in the formulation creates a less favorable environment for microbial growth due to lower water activity. Texture profile analysis: This analysis was performed to stimulate the action of human finger touching the surface of the product formulation. Through visual inspection and touch, texture of S10 masker is thicker, emollient and firmer than the commercial mud mask. The texture of CF is thinner, softer and rough when spread. Observed attributes for both S10 and CF are given in Table 10.

TABLE 10. Texture profile analysis.

Attributes	S10	CF
Hardness cycle 1 (g)	648.67 ± 91.44	3614.33 ± 279.53
Hardness cycle 2 (g)	686.00 ± 197.76	3407.67 ± 346.79
Resilience	0.05	0.04
Adhesiveness (Pa)	0.73 ± 0.06	0.92 ± 0.06

Note: The value presented in mean ± standard deviation (n=3); g: grams; Pa: Pascals

Hardness measures the firmness at specific depth and the energy needed to attain a given deformation to define depth during the first compression cycle (hardness cycle 1) and during lifting which is read as hardness cycle 2. Adhesiveness is the trait of stickiness resembling work needed to overcome the attractive force between sample and probe. Based on Table 10, the hardness measured during cycle 1 and 2 of S10 (648.67 g ± 91.44 g; 686.00 ± 197.76 g) is lower than CF (3614.33 g ± 279.53 g; 3407.67 ± 346.79 g). This implies that CF's texture is firmer than S10. However, S10 is easier to spread and less sticky compared to CF based on the lower adhesiveness reading. Both S10 and CF (commercial) samples displayed almost similar resilience reading which denotes ability of the product to regain its original shape and size.

FTIR analysis: The spectra of selected samples (S9, S10, S11, and S12) in comparison to water and CF are presented in Figure 7. In general, the major -OH peak stretch of alcohols attributed to water can be found in the 3200-3600 cm^{-1} region with the maximum observed at 3300-3400 cm^{-1}. The main aim was to ascertain the presence of water in the selected prepared samples. The most intense water notation based on transmittance % was seen in CF (having

aqua or water as its ingredients), followed by S11, and S9. The intensity was lower in S10 and S12. This observation confirmed S10 as the best waterless masker formulation. Usually there will be three peaks for water. The peak at 3200 cm^{-1} corresponds to the complete hydrogen bonding between water molecules in tetrahedral coordination, the peak at 3400 cm^{-1} refers to incomplete tetrahedral hydrogen bonding, and the peak at 3600 cm^{-1} denotes free OH stretching or weak hydrogen bonding [31, 32].

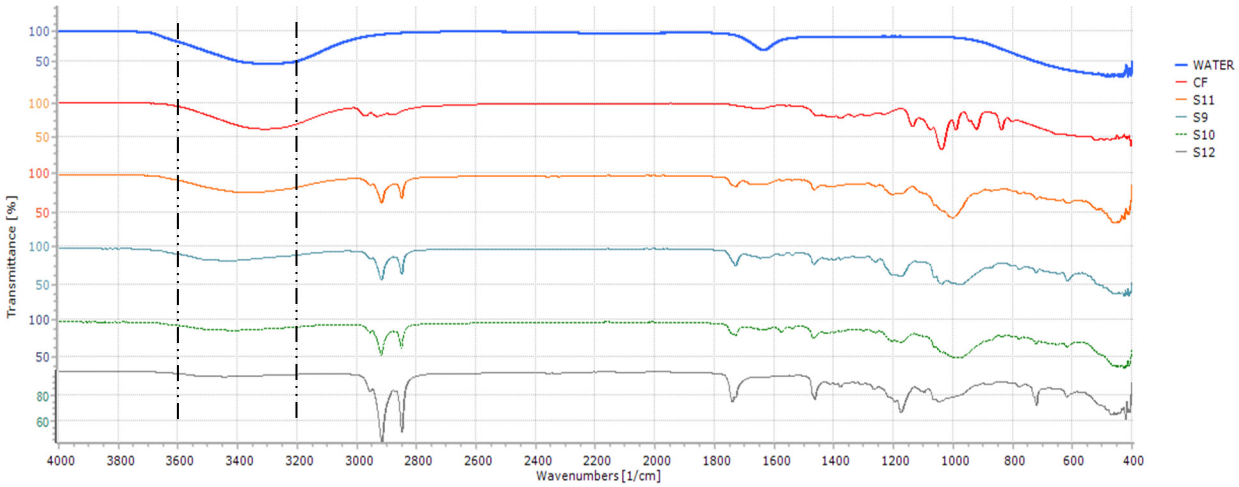

FIGURE 7. FTIR spectra of water, CF, S9, S10, S11, and S12.

Cleansing Test

Figure 8 portrays the cleansing test observation as part of functionality evaluation. The removal of MF from skin surface by rubbing showed that NBC was more effective as it required only half the effort (27 rubs) compared to just water (53 rubs). The addition of NBC provided the extra scrubbing effect and adsorption ability. The test when repeated with the masker formulation also gave similar outcome. The effectiveness of S10 was evaluated for the removal of lipstick stain and MF, and compared to water. The number of rubs and after effect were noted. S10 required a lesser number of rubbings (30), with cleaner after wash effect compared to washing with only water. Based upon the observation, both water, NBC, and S10 had the ability to remove and cleanse MF through rubbing. However, NBC and S10 (masker formulated with the inclusion of NBC) showed better cleansing and after rinse skin feel effect compared to water only.

Cleansing agent		Observation and outcome	
(a) Water	 MF	 No. of rubs = 53 with 15 drops of water	 After: not clean, MF leftover, dry feel.
(b) Water	 MF	 No. of rubs = 72 with 10 drops of water	 After: not clean, MF leftover, dry feel.
(c) NBC	 MF	 No. of rubs = 27 with 6 drops of water	 After: Clean and easy to rinse.
(d) S10	 Lipstick stain	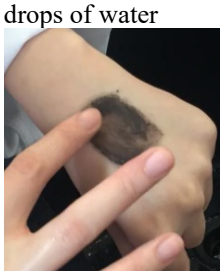 No. of rubs = 30	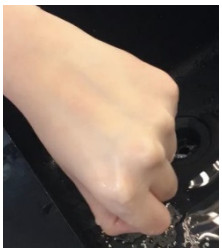 After: Clean and easy to rinse.
(e) S10	 MF	 No. of rubs = 30	 After: Clean and easy to rinse, emmollient feel.

FIGURE 8. Cleansing of (a) MF with 15 drops of water, (b) MF with 10 drops of water, (c) MF with NBC, (d) lipstick stain with NBC based masker formulation (S10), and (e) MF with NBC based masker formulation (S10).

In the color removal test (Figure 9), MF was hard to remove from the glass slide with only water. Even if MF was no longer noticeable, its oily stains and residues were still evident. This may be due to the oil and water-resistant constituents of the MF. Nonetheless, after rubbing under flowing NBC suspension or water, the residues left on the glass slide seemed easier to be removed when pressed lightly with tissue. The MF stains were easily transferred onto the tissue when they were pressed together. From the experiment, makeup stains that have been rubbed with NBC suspension were much easier to be wiped off with tissue than the makeup stains that have been rubbed with only water. This can be attributable to the attraction of MF towards NBC and eventually becomes attached and effortlessly adsorbed. These produced a stable complex. When wiped off with tissue, the NBC particles were transferred to the tissue together with the foundation makeup, making cleansing much easier with far less effort.

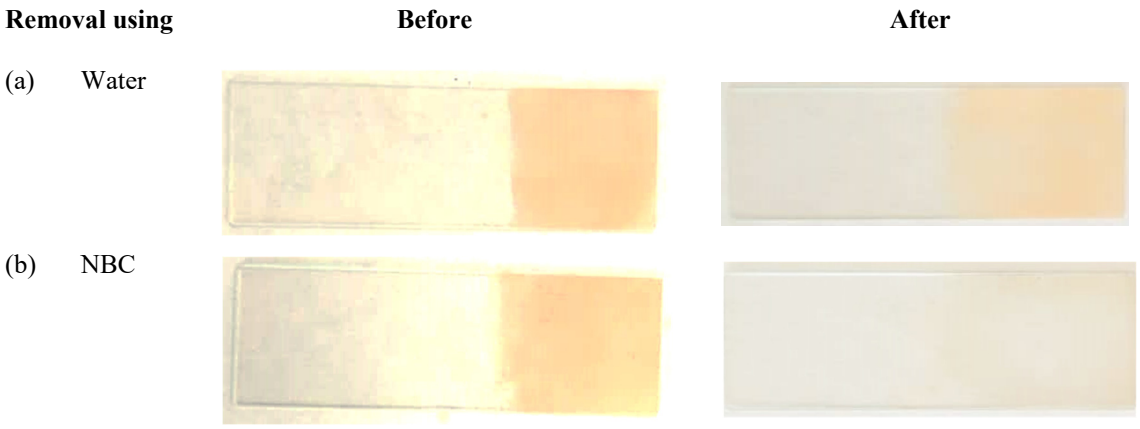

FIGURE 9. Color removal test, (a) with water; (b) with NBC.

The colorimetry analysis was conducted using CIE L*a*b* coordinates to measure the residual color and color differences between water rinsed and NBC rinsed sample glass slides (Table 11). CIE L* a* b* coordinates were used as color-opponent, stated that two colors cannot be yellow and blue, red and green at the same time. L* represent lightness, an increase in the value of L* meant that the sample has become lighter, and darker if the value of L* decreased. Coordinate a* indicates red or green color. As the value increases, the sample is redder and if it decreases, the sample becomes greener. Coordinate b* represents yellow or blue. If the sample is yellower, the value is higher and if its bluer, the value is lower. In this experiment, only lightness + (L*), redness + (a*) and yellowness + (b*) were measured since foundation shades are based on redness and yellowness.

TABLE 11. Color analysis.

	Sample	No.	Color coordinate (before)			Color coordinate (after)			Total color differences			
			L*	a*	b*	L*	a*	b*	ΔL*	Δa*	Δb*	ΔE*
(a)	Water	1	45.75	6.55	13.90	50.85	4.52	12.05	5.1	-2.03	-1.85	5.79
		2	42.78	4.19	10.21	51.60	3.94	9.59	8.82	-0.25	-0.62	8.85
		3	46.27	5.54	12.86	45.26	4.49	11.37	-1.01	-1.05	-1.49	2.08
(b)	NBC	1	43.31	5.60	12.43	53.64	2.94	7.17	10.33	-2.66	-5.26	11.89
		2	44.99	6.12	13.34	52.15	2.96	6.91	7.16	-3.16	-6.43	10.13
		3	43.54	5.22	12.19	52.90	3.20	8.03	9.36	-2.02	-4.16	10.44

Table 11 also shows that there is a significant difference in color for before and after test based upon the total color differences (Δ). Overall, ΔL* had increased in value which indicated that MF had become lighter in color. The magnitude of ΔL* was higher and more consistent with NBC. Decreased difference value of a* (Δa*) and b* (Δb*) reflects the reduction in redness and yellowness intensity. The magnitude was higher with the use of NBC suspension. Increase in lightness and reduced redness and yellowness imply MF removal. The difference in overall color change (ΔE*) was also higher and more consistent with NBC (11.89, 10.1,3 and 10.44) as opposed to water (5.79, 8.85, and 2.08). This showed that NBC has the ability to adsorb and remove color from MF. NBC had also been shown to adsorb

up to 99% of methylene blue (5 mg/L) over a period of 20-30 min (unpublished data). The inclusion of NBC in skincare and makeup remover products would certainly be advantageous.

Makeup removal depends on the makeup formula composition and makeup remover formulation (micelle structure). During makeup removal, force from the skin rubbing will disrupt the microemulsion of the makeup remover which contains water-in-oil (w/o) micelle [33]. This will cause the oil and surfactants of the remover to aggregate with the makeup on skin forming micelles which will then be displaced by water during rinsing. Based from the observation and test, the removal of lipstick and MF from skin surface by rubbing with S10 was highly effective. Reduced number of rubs were needed. The skin was cleaner, and felt cleaner resulting from scrubbing and adsorbing cleansing factor of NBC, while emollient after effect feel is from the masker's active ingredient benefit. The ingredients used and their function in the formulation of the waterless masker is described in Table 12 [34].

TABLE 12. The masker ingredients and their function.

Ingredients	Some beneficial functions
Shea butter	Emollient, moisturizer
Mango butter	Emollient, moisturizer
Olivem 1000	Emulsifier, non-gelling thickener, improves skin barrier integrity
Grape seed oil	Emollient, moisturizer, heal acne, protection against free radicals
Cetyl alcohol	Co-emulsifier, non-gelling thickener
Rhassoul clay	Skin impurities clearing, skin lightening, nourishing, firming, Exfoliator, scrub effect
Sodium cocoyl isethionate	Mild cleansing agent, surfactant
Spa fine salt	Detoxifying, Exfoliator, scrub effect
Rose extract	Moisturizer, hydrating, anti-aging, anti-irritant, antiseptic, anti-inflammatory, antioxidant
Glycerine	Emollient, humectant, skin softening, skin repairing
Beeswax	Emollient, emulsifier, non-gelling thickener, humectant, moisturizer
NBC	Multifunctional (detoxifying, adsorbent, exfoliator, scrub effect)

Among consumers, there are concerns over the use of harsh ingredients such as mineral oil, surfactant, silicone resins or hydrophobic polymers in many commercial makeup removers [35, 36]. The inclusion of these substances often necessitated by the need to reduce cost, enhance waterproof properties, and to produce effective makeup remover. In this study, the ingredients chosen (Table 12) were the ones that are non-irritant, noncomedogenic in nature or low on the comedogenic scale rating (< 3). Grapeseed oil for example (rating of 1), can help improve skin barrier and reduce the appearance of acne scars and hyperpigmentation, and suitable for all skin conditions and types.

The inclusion of NBC in masker formulation was proven practical and effective. S10 formulation mix had the most preferrable properties and characteristics to be further developed as a full-fledged multifunctional skincare product. These findings suggest that NBC can be used in masker and other commercially potential charcoal-based product formulations.

Sustainability in beauty emphasizes on areas such as waterless beauty, upcycling, carbon neutrality, and reusable or refillable packaging solutions [37]. The waterless beauty approach is popular with manufacturers whom are exploring ways to reduce [4] or remove water [38] from their product formulations to be more environmentally conscious. Solid concentrated formats can have a lower cost per use compared to traditional water-based formats. Future work will focus on powder and stick products which can be formulated without water and easy for on the go use during travelling. The absence of water increases ingredients stability as with those that spoil or oxidize easily. The use of NBC in combination with other natural ingredients can be further explored.

Key interests in the anti-pollution beauty market are mostly directed to cleansing clay masks, balancing toners, deep cleansing products, and natural oil-based cleansers [6]. The trend is fast gaining momentum not only in Asia but across Europe and North America. The biocarbon material will be beneficial in the development of biocarbon enriched personal care products for the local market. Iron oxides are even well tolerated by those with sensitive skin. Here we incorporate active biocarbon composite in masker formulations to take up the anti-pollution skin care theme. Adsorption capability can be seen as advantageous in developing skin care products for cleansing and detoxifying. Apart from being an adsorbent, NBC can function as natural exfoliants with scrubbing effect that can facilitate in the removal of dead epidermis cells.

Lifestyle demand will support the growth of anti-pollution skincare products as consumers become more self-conscious towards skin health. The market can be categorized into face masks, cleansers, moisturizers, creams, and others. As more people are on the go nowadays. More people have the notion that they have less time than before. More people seek a safer, effective, more convenient, more functional 'all in one' product as a better solution for customer satisfaction. This resonates the change in consumer's need, lifestyle, and preference for products that optimizes time, effort, and money. It would be best to formulate and develop a multifunctional product such as a masker that can function as a facewash, cleanser, and makeup remover with scrubbing and exfoliating effect as well. Together with its moisturizing and soothing effect, it can help towards healthier skin rejuvenation.

There have been less reports locally on the utilization of agrobiomass derived biocarbon in repurposing the material for producing higher added value product derivatives. This work had demonstrated the potential of agrobiomass derived biocarbon composites as high value-added product for use in the formulation of personal care products. This will indirectly support the cause towards environmental sustainability. More ventures into low cost, low value biomass feedstock can be explored as to drive value-added biocarbon entry into mainstream market product inclusion.

CONCLUSION

The synthesis of a laboratory developed new active biocarbon composite (NBC) has been successfully performed. The composite consists of a mix of carbonized hard (coconut shell), soft (leaf), and modified biomass material. Initial adsorption test proved the practicality of NBC for use in personal and skin care. The following optimum parameters in MF removal were identified, i.e., adsorbent dosage (0.028 g), makeup foundation concentration (up to 300 mg/L), particle size (151-300 μm), and contact time (15 min). Later, NBC was used in the formulation of a waterless charcoal-based masker. Coupled with the adsorption capability of NBC, the newly formulated masker (S10) displayed promising functionality and acceptable properties (pH, color, odor, texture, gentleness, and rinseability) for use in skin care. Blending-in of NBC into various personal care product formulation such as cleansing balm, clay mask, face scrub, and shampoo can raise the competitiveness of local product line.

ACKNOWLEDGMENTS

This project was supported by the Ministry of Higher Education Malaysia, through PPRN 2.0 grant (R/PPRN/A07.00/01397A/006/2019/00678) and our industry partner, I Medikel Cosmeceutical (M) Sdn. Bhd.

REFERENCES

1. L. Wood, *Global Beauty and Personal Care Market Report 2021-2026* (https://www.researchandmarkets.com/r/oyrzqf, 2021).
2. T. Yeoh, *Malaysia Beauty and Personal Care* (https://www.trade.gov/market-intelligence/malaysia-beauty-and-personal-care, 2021).
3. S. K. Cheong, J. Coulthart, J. Kanawati, A. Han, J. Li, P. Maryarini, C. Ono, M. Pookan, D. Robles, Y. Rumeral, S. Sherigar, S. Yan, T. Yeoh, L. Theseira and H. Baik, *Asia Personal Care & Cosmetics Market Guide* (Department of Commerce, International Trade Administration, USA, 2016).
4. N. Lionetti, Cosmetics & Toiletries. **136**, 52–58 (2021).
5. Infinium, *Anti-Pollution Skin Care Products Market* (https://www.infiniumglobalresearch.com/consumer-goods-packaging/global-anti-pollution-skin-care-products-market, 2021).
6. B. Schleehauf, *Cosmetics & Toiletries*, (https://www.cosmeticsandtoiletries.com/marketdata/segments/The-Ingredients-Driving-the-Anti-pollution-Beauty-Market-511783742.html, 2019).
7. M. Picard, S. Thakur, M. Misra, D. F. Mielewski and A. K. Mohanty, Sci. Rep. **10**, 3310–3323 (2020). https://doi.org/10.1038/s41598-020-59582-3.
8. P. Quosai, A. Anstey, A. K. Mohanty, and M. Misra, R. Soc. Open Sci. **5**, 171970–171975 (2018). http://dx.doi.org/10.1098/rsos.171970.
9. A. Nor Asfaliza, P. Sannasi, M. A. Mohamad Faiz and Z. Nor Azah, Mater. Today. **5**, 21888–21896 (2018).
10. K. Ataman, *Cyclopentasiloxane* (https://www.ataman-chemicals.com/en/products/cyclopentasiloxane-1235.html, 2020).

11. W. Johnson Jr, W. F. Bergfeld, D. V. Belsito, R.A. Hill. C.D. Klaassen, D.C. Lieber, J. G. Marks Jr, R.C. Shank, T. J. Slaga, P. W. Synder and F. A. Andersen, Int. J. Toxicol. **30**, 149S–227S (2011). https://doi.org/10.1177/1091581811428184.
12. Focallure, *Skin Evolution* (https://focallure.com/collections/face-makeup/products/focallure-skin-evolution-liquid-foundation, 2019).
13. P. Sannasi, A. Huda and B. Jayanthi, Pertanika J. Sci. Technol. **29**, 427–444 (2021).
14. R. Wannahari, P. Sannasi, M.F.M. Nordin and H. Mukhtar, ARPN J. Eng. Appl. Sci. **13**, 1–9 (2018).
15. P. Sannasi, H. F, Chau and M. H. Nuramira Najua, J. Eng. Appl. Sci. **12**, 2449–2460 (2017).
16. T. Shahnaz, V. Sharma, S. Subbiah and S. Narayanasamy, J. Water Process. Eng. **36**, 1010283 (2020). https://doi.org/10.1016/j.jwpe.2020.101283.
17. D. J. Davies, J. R. Heylings, T. J. McCarthy and C. M. Correa, Toxicol. In Vitro. **29**, 176–181 (2015).
18. R. M. Walters, G. Mao, E. T. Gunn and S. Hornby, Dermatol. Res. Pract. **2012**, 3–9 (2012). https://doi.org/10.1155/2012/495917
19. T. Kishina, K. Kaneko, A. Tatsuta, Y. Sato, M. Shudo, M. Yamaguchi, H. Usuki, M. Nosaka and N. Takeshita, US Patent No. 9968542 B2 (2018).
20. I. Victor and V. Orsat, J. Food Sci. Technol. **55**, 3845–3849 (2018).
21. M. Rayma, *Humblebee & Me* (https://www.humblebeeandme.com/sea-buckthorn-and-charcoal-cleansing-balm, 2018).
22. R. P. Vieira, A. R. Fernandes, T. M. Kaneko, V. O. Consiglieri, C. A. S. O. Pinto, C. S. C. Pereira, A. R. Baby and M. V. R. Velasco, Braz. J. Pharm. Sci. **45**, 515–525 (2009).
23. C. C. Nnaji and S. C. Emefu, J. Bioresour. **12**, 3123–4145 (2017).
24. Y. Chen, J. Shi, Q. Du, H. Zhang and Y. Cui, RSC Adv. **9**, 14143 (2019). https://doi.org/10.1039/C9RA01271K
25. Thermo Fisher Scientific, *Knowledge Based, Infrared Spectral Interpretation* (Thermo Fisher Scientific Inc, 2009).
26. C. Anyika, N. A. Mohd Asri, Z. Abdul Majid, A. Yahya and J. Jaafar, Nanotechnol. Environ. Eng. 2:16 (2017). https://doi.org/10.1007/s41204-017-0027-6.
27. M. Jain, M. Yadav, T. Kohout, M. Lahtinen, V. K. Garg and M. Sillanpää, Water Resour. Ind. **20**, 54–74 (2018).
28. J. Ríos-Hurtado, E. Múzquiz-Ramos, A. Zugasti-Cruz and D. Cortés-Hernández, J. Biomater. Nanobiotechnol. **7**, 19–28 (2016). doi: 10.4236/jbnb.2016.71003.
29. C. R. Laili, S. Hamdan, M. Mazidah and Z. L. Thang, AIP Conference Proceedings **1885**, 020113, (2017). https://doi.org/10.1063/1.5002307.
30. S. Wong, N. A. N. Yac'cob, N. Ngadi, O. Hassan and I. M. Inuwa, Chin. J. Chem. Eng. **26**, 870–878 (2018). https://doi.10.1016/j.cjche.2017.07.015.
31. F. Cheng, Q. Cao, Y. Guan, H. Cheng, X. Wang and J. D. Miller, Int. J. Miner. Process. **122**, 36–42 (2013).
32. J. J. Max and C. Chapados, J. Chm. Phys. **127**, 114509-1–114509-10 (2007).
33. N. Pakkang, Y. Uraki, K. Koda, M. Nithitanakul and A. Charoengsaeng, J. Surfactants Deterg. **21**, 809–816 (2018).
34. L. Meena, *Personal Formula Resources*, (https://www.personalformularesources.com/shop/ingredients/, 2019).
35. L. Chularojanamontri, P. Tuchinda, K. Kulthanan and K. Pongparit, J. Clin. Aesthet. Dermatol. **7**, 36–44 (2014).
36. E. J. Kim, B. J. Kong, S. S. Kwon, H. N. Jang, S. N. Park, J. Cosmet. Sci. **36**, 606–612 (2014).
37. A. Fisher, *Sustainable Skin Care in 2021 and Beyond,* (https://www.mintel.com/blog/beauty-market-news/sustainable-skincare-in-2021-and-beyond, 2020).
38. S. Bauer, *Everything You Need to Know About the Waterless Beauty Trend*. (https://www.shape.com/lifestyle/beauty-style/waterless-beauty-products, 2020).